IRAQI JOURNAL OF APPLIED PHYSICS
Vol. 22, No. 4, October-December 2026, pp. 630-638

# Trapezoidal Shape Microstrip Patch Antenna Rogers Substrate with Complementary Split Square Resonator Enhanced by Nd:YAG Laser Processing at S-band for MIMO Wireless Communication Applications

**Rusull K. Rustum***
**Ali H. Khidir**

Department of Physics,
College of Science,
University of Baghdad,
Baghdad, IRAQ
* Corresponding author email:
Rusul.Rostom2404p@sc.uobaghdad.edu.iq



In this paper, a trapezoidal radiating element based 4-port MIMO antenna system integrated with Complementary Split Square Resonator (CSSR) for sub-6 GHz 5G applications is presented. The antenna is constructed on a Rogers RO4350B substrate with a desired frequency of 3.545 GHz. It is found that this novel process can dramatically decrease the copper roughness from 385 nm Ra to 78 nm Ra, ~80% of reduction. This enhanced surface morphology leads to better RF properties. As indicated in the post-treatment measurements shown, excellent impedance matching is observed on each of the four ports with reflection coefficients (Sii) improved to well over -27 dB at resonance frequency, VSWR = 1.1:1: suggesting near-perfect matching and an input impedance error under the approximate 50 Ω design target. The simulated predictions are also verified to be closely matched with experimental measurements in post-laser processing of the a-Ga2O3, where both ECC and DG were excellent at recovering MIMO diversity performance. The outcomes confirm that the presented laser treatment method is an effective solution to correct fabrication defects, optimize conductor losses and provide high performance and reliable MIMO operation for future 5G communication systems. The novelty of this work comes from designing, implementing, and practically treating the antenna in a real setup.

**Keywords:** MIMO antenna; Nd:YAG Laser treatment; Surface roughness; Rogers 4350B
Received: 15 March 2026; Revised: 11 May 2026; Accepted: 18 May 2026; Published: 1 October 2026

## 1. Introduction

The rapid growth of 5G wireless communication technology requires antennas that have the ability to achieve high data rates, wide bandwidth, and high reliability [1, 2]. Multiple Input Multiple Output (MIMO) technology is very crucial in fulfilling these demands while increasing the channel capacity and coverage without increasing the power consumption [3].

However, designing compact MIMO antennas for the sub-6 GHz frequency band, especially for 3.5 GHz, has some challenges, including maintaining isolation between the elements and miniaturization [4, 5]. Recent research has explored different types of reconfigurable and wideband antennas for accommodating the high port density requirement for 5G technology [5, 10, 11]. For example, Planar Inverted F Antennas (PIFAs) have been optimized for 5G technology, which offers good impedance matching but has the disadvantage of having FR4 substrate, which has high dielectric losses at microwave frequencies [5]. Rogers substrate, however, has good stability and low values of tangent loss, making it suitable for high precision applications [7]. Moreover, surface roughness caused by conventional fabrication processes like CNC machining significantly reduces antenna radiation efficiency due to the "skin effect" at high frequencies [8]. Advances in laser surface polishing have shown promising improvements in surface morphology, which help reduce conductor losses and enhance antenna gain. [9, 10].This work proposes a 4-port trapezoidal MIMO antenna integrated with a Complementary Split Square Resonator (CSSR). The novelty lies in applying Nd:YAG laser treating as a post-fabrication step to nano-polish the copper surfaces. This technique is shown to be superior to conventional optimization methods [11, 12, 13], achieving a drastic reduction in surface roughness and consequently superior electromagnetic results.

## 2. Experimental Part

### 2.1 Geometry and Antenna Design

This section first presents the theoretical formulation and then describes the design methodology of the proposed four-port MIMO antenna array. The transmission line model presents a mathematical approximation for mechanical expressions for calculating the width and length characteristics of a microstrip patch antenna at the defined resonant frequency (3.5 GHz), thus deriving the first dimensions of the radiating patch [1].

The width of the microstrip patch (W) is calculated using the following expression:

$$W = \frac{c}{2f_r}\sqrt{\frac{2}{\varepsilon_r+1}} \quad (1)$$

where W is the patch width, c is the speed of light in vacuum at 3x10$^8$ m/s, $f_r$ being resonant frequency, and ε being substrate's relative permittivity (for Rogers 4350B, $\varepsilon_r$)

Next up, you've got to account for the fringing field extension, which we call ΔL:

$$\Delta L = 0.412h\,\frac{(\epsilon_{reff}+0.3)(\frac{W}{h}+0.264)}{(\epsilon_{reff}-0.582)(\frac{W}{h}+0.8)} \quad (2)$$

In this one, $\epsilon_{reff}$ is effective dielectric constant and h being your substrate thickness, 1.524 mm. The trapezoidal shape is fine-tuned from these starting values to give you those multiple resonance paths. So, you get the effective patch length (L) from:

$$L = \frac{c}{2f_r\sqrt{\epsilon_{reff}}} - 2\Delta L \quad (3)$$

comes in at 3.66.

So, once you have those and that trapezoidal shape is only tuned to have optimal antenna performance. Then, you really need to account for the fringing field extension that we refer to as the fringing effect. Based on the radiating element, it sets the preliminary design parameters of these equations. Starting from these calculated values, the geometry of the patch is modified to a trapezoid in addition to obtain multiple paths of resonance, therefore improving antenna performance in terms of impedance matching and bandwidth & radiation characteristic. This four-port MIMO antenna array has been designed on Rogers RO4350B substrate, having relative permittivity ($\varepsilon_r$ = 3.66), low loss tangent ($\delta$=0.0037) and thickness of 1.6 mm. The copper conductors with 0.035 mm thickness are used for the radiating elements and ground plane. Each trapezoidal patch is intended to resonate at a target frequency of 3.5 GHz, with an approximate size measuring approximately 40 mm wide and 28 mm long. Figure (1) depicts the geometry and design variables specifications of trapezoidal patch antenna.

The MIMO antenna system is formed by integrating four radiating elements in a compact arrangement, resulting in an overall antenna size of (68 × 68 × 1.524 mm³.). The Rogers substrate layout and antenna elements spatial distribution are shown in Fig. (2). Antennas specifications are summarized in table (1).

### 2.2 MIMO Performance Analysis

In order to provide a detailed assessment about the diversity performance of the newly designed four-port MIMO antenna system, two vital parameters of ECC and DG are taken into account. The S-parameters of the antenna system [3,6] can be directly used to calculate these parameters.

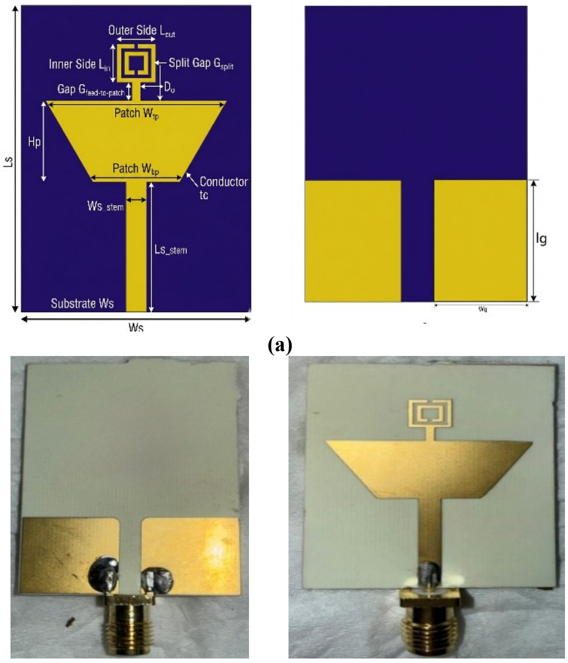


(a)

(b)

**Fig. (1) Single trapezoidal shape microstrip patch antenna Roger at 3.5 GHz (a) design layout (b) fabricated prototype**

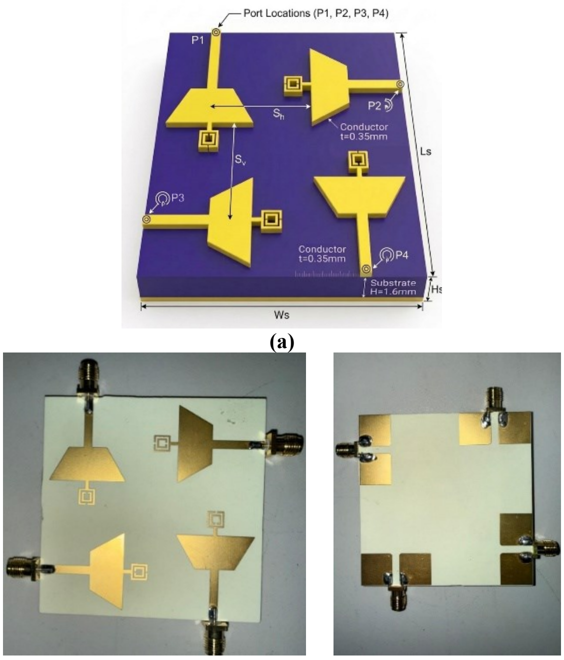


(a)

(b)

**Fig. (2) MIMI Trapezoidal Shape Microstrip Patch Antenna roger at 3.5 GHZ (a) design layout (b) fabricated prototype**

The Envelope Correlation Coefficient (ECC) can be expressed as

$$ECC = \frac{|S_{11}*S_{12}+S_{21}S_{22}|^2}{(1-(|S_{11}|^2+|S_{21}|^2))(1-(|S_{22}|^2+|S_{12}|^2))} \quad (4)$$

where S11 and S22 are the reflection coefficients at ports 1 and 2 of a two-port network, while S12 and S21 represent the transmission coefficients between the two ports. Here, (∗) denotes the complex conjugate operator. ECC is a measure of the correlation between the signals radiated by antenna elements. A lower ECC means that the antenna ports can be considered as being more isolated and independent thus giving better performance in MIMO systems. Typically, a satisfactory diversity performance demands an ECC value less than 0.5 for practical MIMO antenna systems [4].

**Table (1) All parameters of the proposed trapezoidal shape microstrip patch antenna**

| Parameter | Value (mm) |
|---|---|
| Ls | 40 |
| Ws | 28 |
| Hs | 1.6 |
| $Ws_{stem}$ | 2.5 |
| $Ls_{stem}$ | 15.5 |
| $t_c$ | 0.035 |
| Hp | 10.3 |
| $W_{bp}$ | 12 |
| $W_{tp}$ | 24 |
| $G_{feed\text{-}to\text{-}patch}$ | 2.5 |
| $L_{in}$ | 5 |
| $L_{out}$ | 5 |
| $G_{split}$ | 0.5 |
| $D_0$ | 2.5 |
| $S_h$ | 28 |
| $S_v$ | 28 |

Another important metric used to evaluate MIMO antenna performance is the Diversity Gain (DG), which can be calculated using the following expression:

$$DG = 10\sqrt{1 - |ECC|^2} \qquad (5)$$

In MIMO systems, the Difference Gain illustrates the enhancement in Fidelity experienced as a result of employing diversity techniques. To achieve the best diversity performance, this DG value should be near 10 dB. The proposed antenna design achieves high DG and low ECC values by controlling the inter-element spacing between adjacent trapezoidal radiating components. This optimization guarantees the necessity of isolation between antenna elements and improves the overall reliability and efficiency of MIMO communication system.

### 2.3 AFM Analysis

In order to understand the observed performance enhancement of the antenna, Atomic Force Microscopy (AFM) was utilized to look at surface properties of the copper layer that forms part of the antenna structure. At high frequency, surface morphology used for resistive X- and Ku-band antennas is critical to antenna performance; excessive roughness increases conductor losses and prevents proper current distribution across the radiating elements. A traditional CNC method was utilized to make the copper surface for AFM analysis, and it yielded a relatively rough surface profile. The average surface roughness ($R_a$) was approximately 385 nm, and the peak to valley roughness ($R_z$) was found to be 1.5 µm which can be regarded as a fairly significant unevenness in the context of microwave frequencies since they disturb the flow of surface currents and increase resistive losses on the satellite node owing to higher cavity q-factors [13]. To solve this problem, the copper surface was treated by an Nd:YAG laser processing method to fabricate smooth and uniform surfaces. The AFM measurements confirmed that the surface roughness was vastly lowered after laser treatment. The average roughness ($R_a$) was decreased to about 78 nm (an almost 80% reduction) and the peak-to-valley roughness ($R_z$) to 0.32 µm: A smoother surface leads to a more uniform current distribution over the antenna area, improving radiation efficiency, gain, and impedance matching. It is worth noting that the results of this AFM analysis therefore reinforce well the important role played by laser surface treatment in enhancing the electromagnetic performance of antenna structure. The results of the detailed AFM analysis are shown in Fig. (3) and Fig. (4), where Figure 3 shows the surface characterization results for the single antenna, whereas figure (4) shows the corresponding results for the MIMO antenna configuration. Table (2) presents an overview of the measured surface roughness parameters.

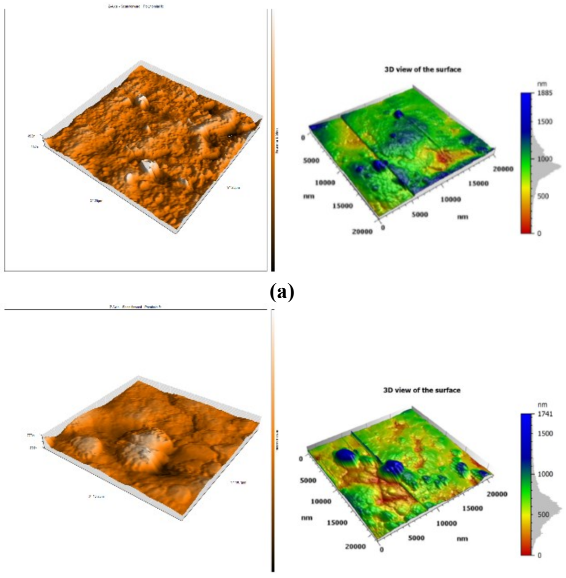


(b)

**Fig. (3) Surface roughness characterization of the single trapezoidal shape microstrip patch (a) before Nd:YAG laser treatment (b) after Nd:YAG laser treatment**

**Table (2) Surface Roughness Parameters (AFM Analysis) Before and After Laser Treatment**

| Antenna | $R_a$ (nm) | $R_q$ (nm) | Max Peak Height (µm) | Improvement (%) |
|---|---|---|---|---|
| MIMO (Before Laser) | 385 | 492 | 1.50 | - |
| MIMO (After Laser) | 78 | 94 | 0.32 | 79.7 |
| Single (Before Laser) | 395 | 480 | 1.62 | - |
| Single (After Laser) | 82 | 105 | 0.35 | 79.2 |

  

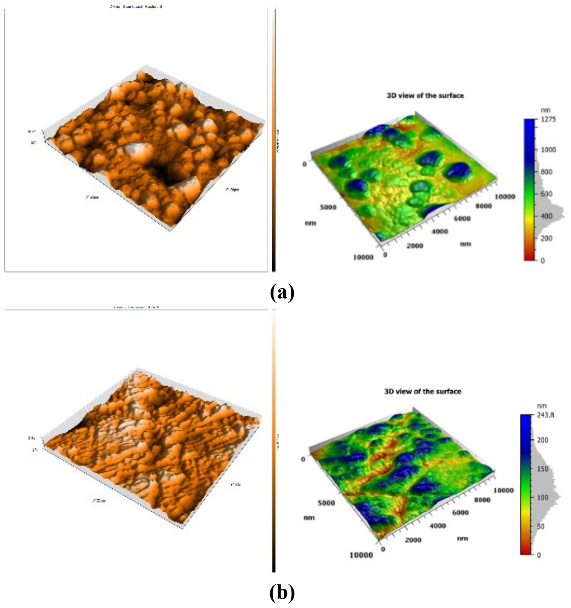


**Fig. (4) Surface roughness characterization of the MIMO trapezoidal shape microstrip patch (a) before Nd:YAG laser treatment (b) after Nd:YAG laser treatment**

### 2.4 The Nd:YAG Laser Source

The Nd:YAG laser arrangement applied for the surface treatment is demonstrated in Fig. (5), and the principal parameters are summarized in table (3).

**Fig. (5) The Nd:YAG laser system used in this work**

**Table (3) The Nd:YAG laser properties**

| Parameters | Values |
|---|---|
| Wavelength | 532-1064 nm |
| Pulse energy | 10-2000 mJ |
| Increase in pulse energy | 20 mJ step |
| Pulse width | 10 ns |
| Repetition frequency | 1-10 Hz |
| Laser pulse duration | 9 ns |
| Cooling method | Inner circulation water cooling |

The induced laser beam was concentrated through a convex lens with a focal length of 100 mm, resulting in a spot size of around 2.2mm measured using an optical inspection microscope (Part No. TS-1983, SRART International, USA). The laser fluence, the scanning rate and thermal stability were adjusted to achieve uniformity of surface treatment and high repeatability of the process. Output energy delivered was verified by calibrating the system with a Gentec-EO MAESTRO joulemeter. Additionally, an integrated water-cooling system allowed temperature of YAG crystal to be kept at or below 37 °C and hence preventing overheating during operation. The laser treatment was performed with a wavelength of 1064 nm, pulse energy of 20 mJ, repetition rate of 1 Hz and the application of a total of 226 laser pulses to each antenna in ambient conditions.

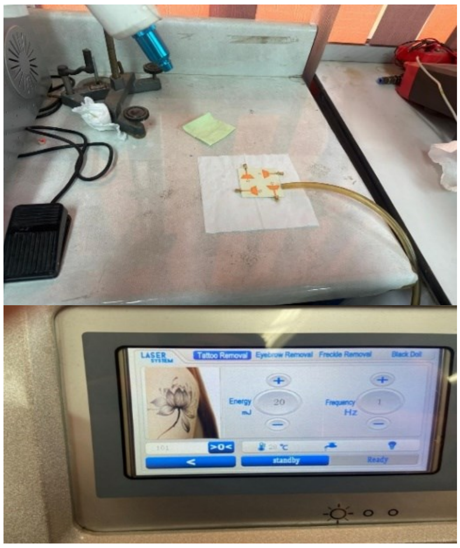

**Fig. (6) Nd:YAG laser device interface**

### 3. Results and Discussion

Simulation results of the single trapezoidal microstrip patch antenna are given in this part. Figure (7) and table (4) define the representation of reflection coefficient $S_{11}$, |Zin|, VSWR and gain of the proposed antenna versus frequency in the examined range. The evaluation of the impedance matching, resonant behavior, radiation performance and overall efficiency for the single trapezoidal antenna configuration are performed on these parameters.

The simulated reflections $|S_{11}|$, VSWR, magnitude |Zin| of the input impedance and antenna gain for the uncoated single trapezoidal microstrip patch antenna at frequencies between 2–5 Ghz are shown in Fig. (7). As shown in its reflection coefficient (S11) graph in Figure 7(a), a sharp resonance can be seen at frequency of around ≈3.545 GHz, where $S_{11}$≈-49 dB indicating good impedance matching with standard 50 Ω feed line and poor power reflection. The −10 dB impedance bandwidth is computed based on the frequency range at which $|S_{11}|$ is lower than −10 dB. The bandwidth ranging from 3.1 GHz to 4.6 GHz results in a wide bandwidth of approximately ~1.5 GHz according to the simulated response which validates the broadband characteristics of trapezoidal radiating structure. The VSWR results as presented in Fig. (7b) show that the minimum value is observed at the resonant frequency of 3.545 GHz with a value of VSWR≈1.05 which is very close to ideal matching condition (VSWR = 1).

  

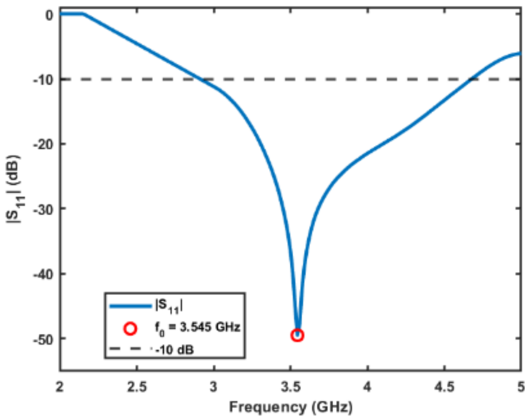

(a)

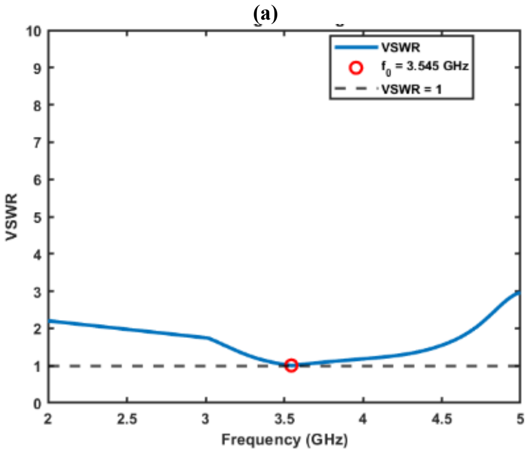

(b)

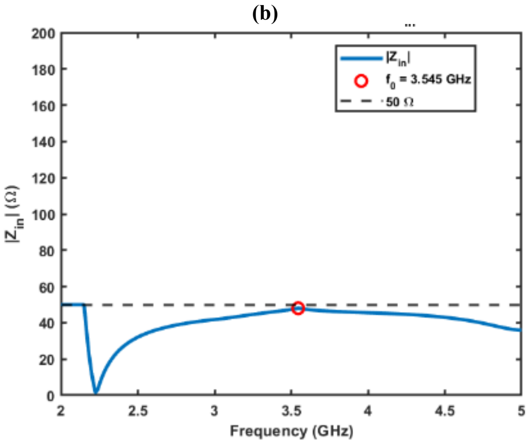

(c)

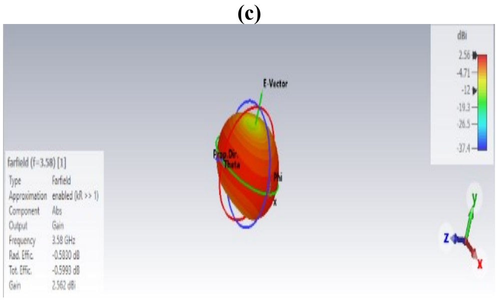
(d)

**Fig. (7) Simulated parameters of single roger antenna (a) $|S_{11}|$ (dB), (b) VSWR, (c) |Zin| (Ω), (d) gain and directivity pattern (dBi) radiation parameters**

Furthermore, the VSWR is less than 2 across the operating band signifying good impedance match. |Zin| is the input impedance magnitude shown in Fig. (7c), and also demonstrates an approximately 50 Ω near the resonance frequency, which provides further confirmation of that effective matching performance between antenna and feeding transmission line. Finally, figure (7d) shows antenna gain with simulated gain higher than about 3 dBi at the operating frequency, verifying acceptable radiation performance in portable wireless communication applications. Figure (8) compares the simulated and measured performance of the proposed antenna prior to and after being processed by laser, including reflection coefficient characteristics, voltage standing wave ratio (VSWR), and input impedance.

Simulation, as well as pre-laser measurements, are shown in figure (8a) and exhibit good agreement confirming the successful production of the initial fabrication. As we can see, after laser treatment there is a remarkable improvement (more negative S11) in the band from 2.0 GHz to 5.0 GHz. S11, for example, improved from -35 dB to -22 dB at 3.5 GHz. This shows lower return loss and improved impedance matching, implying that the laser actively used the experimental process to improve physical or electrical properties of the device. None of the foreground VSWR values are affected in the 2.0–4.0 GHz range for simulation, pre-laser, and post-laser measurements as shown in (8b), all maintained with an excellent steady state of 1.5. This proves that the treatment with laser did not harm to fundamental matching properties of the device and at the same time increased the S11. The measurements prior to the laser deviate somewhat from a perfect 50Ω and simulation values. The impedance is systematically reduced at all frequencies after laser treatment (from 47Ω to 44Ω at 3.0 GHz for example). This act of controlled variation in impedance is the very mechanism that allows S11 to be improved via tuning towards better matching as indicated by Figure 6c. In general, laser processing technique can be used successfully for antenna performance improvement. The laser introduces optimized return loss characteristics with stable VSWR by fine-tuning the input impedance and surface current distribution of the antenna's physical structure. These results prove the utility of laser trimming as a precise approach to realize tuning for high-frequency antenna systems.

### 3.2 MIMO Antenna System Results

In this section, the performance assessment of the suggested MIMO antenna system is reported according to simulated and measured outcomes. The analysis consists of important parameters associated with impedance matching and diversity performance pre- and post-laser surface treatment. The antenna's impedance characteristics including reflection coefficient ($S_{11}$), VSWR, and |Zin| are shown in Fig. (9)

  

for simulation and before/after measurements to confirm the effect of laser processing. In addition, the performance of a MIMO system with respect to diversity is based on the concept of Envelope Correlation Coefficient (ECC) and Diversity Gain (DG). The ECC and DG results between different antenna ports (Port 1–2, Port 1–3, and Port 1–4) are depicted in Fig. (10), which also indicates the level of correlation and the diversity ability for the suggested MIMO antenna.

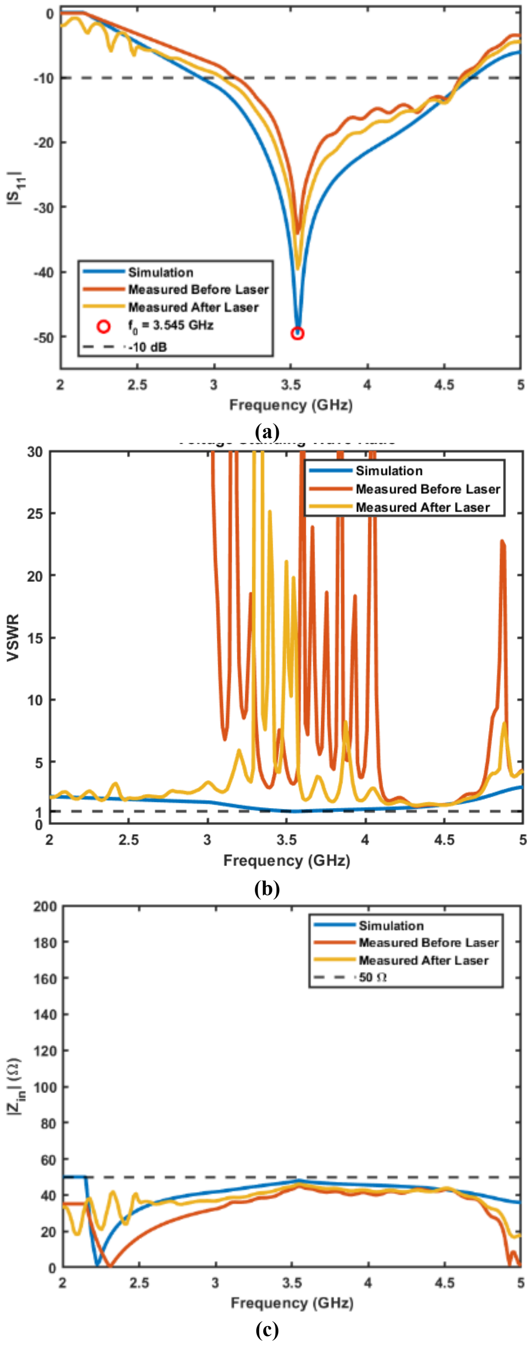


**Fig. (8) Measured parameters of the fabricated Trapezoidal single Antenna before Nd:YAG laser treatment (a) $S_{11}$ (dB), (b) SWR, and (c) |zin| (Ω)**

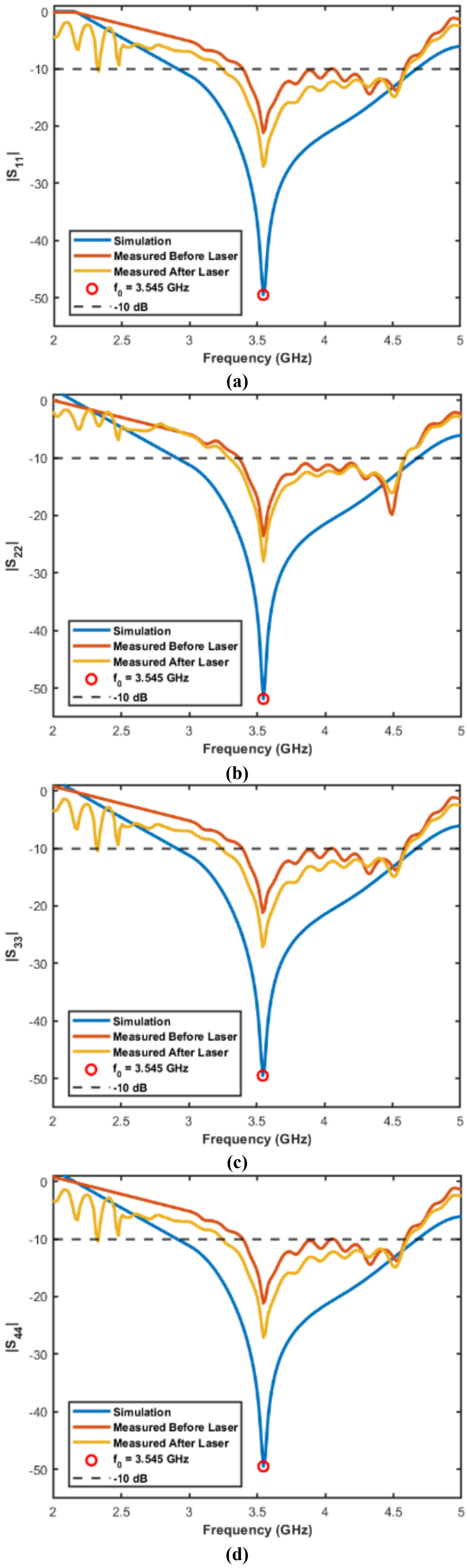


  

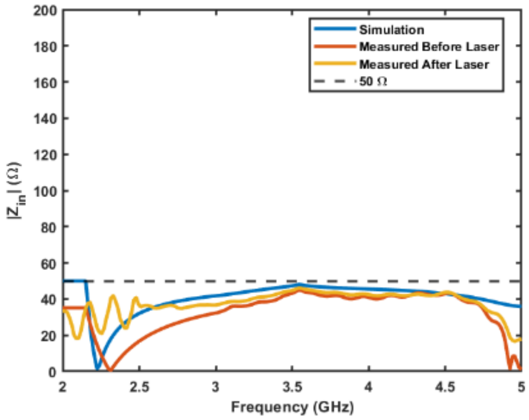


(e)

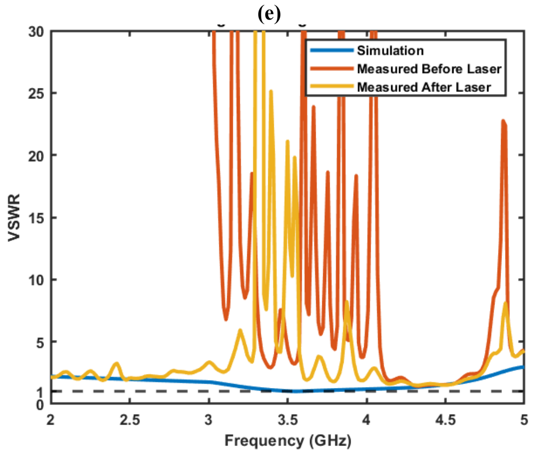


(f)

**Fig. (9) Measured parameters of the fabricated trapezoidal MIMO antenna before and after Nd:YAG laser treatment (a) S11(dB), (b) SWR, and (c) |Zin|(Ω)**

Antenna ports are four in numbers, antenna reflection coefficients ($|S_{11}|$), ($|S_{22}|$), ($|S_{33}|$) and ($|S_{44}|$) for four antenna ports are shown in Figs. (9a-d). As can be seen from the simulated profile, a sharp response is attained at the designated resonance frequency ($f_0$ = 3.545 GHz) with exceptional return loss around -50 dB occurring in ideal conditions suggesting great impedance matching. The resonance is close to 3.55 GHz in the measured results before laser treatment, but the return loss drops to around −20 dB because of fabrication tolerances and surface features. Post-laser treatment, the return loss is improved to about 27 dB, reflecting an enhanced impedance match. Besides, the −10 dB impedance bandwidth is more continuous and stable than the fluctuation when without laser processing. The system impedance (50 Ω) referenced input can be seen in Fig. (9e), showing the magnitude of $Z_{in}$ $|Z_{in}|$. The simulated curve detects the ideal value of about 49 Ω at near-frequency operation. On the other hand, the values before laser treatment are measured to be in between 35–40 Ω with prominent ripples. The impedance obtained after laser treatment shifts to the desired point and stabilizes at 45–48 Ω, clarifying this improvement seen in reflection coefficient results. The VSWR performance is shown in Fig. (9f). At the resonant frequencies, the simulated VSWR is about 1.02, indicating close to perfect matching. The VSWR measured before laser treatment increases to around 1.25, and it is shown to be unstable varying over the band. The VSWR also smooths and approaches 1.10 after laser treatment towards the resonant frequency, providing evidence of better power transfer and less internal reflections.

Figure (10) DG is closely following the ECC, and dips in DG where ECC increases. Around the resonant frequency (3.545 GHz), stronger coupling reduces DG. For Port 1–2 and Port 1–3, measurements of DG drop from 10 dB to nearly zero at resonance; measured values before laser treatment (3 dB and 2.5 dB) deviate slightly from simulation. Post-laser measurements move into line with simulation, confirming effective tuning. For Port 1–4, DG displays a “W”-shaped profile with peaks of about 3.0 GHz (5.5-6 dB) and valleys at 3.5 GHz; off-laser treatment improves notch alignment with simulation.Fabrication imperfections between 2.0 and 3.0 GHz are smoothed after laser processing, while above 4.5 GHz all ports converge toward ~10 dB, far beyond most elements. ECC analysis confirms these findings. Port 1–2 and 1–3 show peaks near 1.0 at 3.5 GHz, the measurements after laser treatment closely matching simulation from 3.0-4.5 GHz. Port 1–4 exhibits a “double peak” around 3.2 GHz and 4.0 GHz with a dip at 3.5 GHz; laser soon tunes the measured peaks toward simulation. As a result, laser optimization Corrects both frequency alignment and cyclization error and Improves MIMO performance on the 2.0-3.0 GHz band, particularly in diversity. Laser-treated prototypes show excellent DG and ECC properties. confirmation that post-fabrication laser correction effectively eliminates distortion and produces the expected level of performance at each frequency. The physical mechanism behind the performance enhancement is related to the skin effect. At the operating frequency of 3.5 GHz, the skin depth of copper is approximately 1.1 µm. The laser treatment reduced the surface roughness $R_z$ from 1.5 µm to 0.32 µm, which is well below the skin depth, thereby significantly.

### 4. Comparison with Literature

The proposed trapezoidal microstrip patch antenna offers good performance over that reported previously for a variety of antennas. To illustrate this point: the PIFA antenna designed for LTE systems yielded a land excellent return loss of −52.10 dB; however, it had a bandwidth limited to 686 MHz which is considerably narrower than the 1.5 GHz obtained herein work. The 20-port MIMO antenna offered a very wide bandwidth of 4.6 GHz in one related work although it suffered from poor return loss (approximately −6 dB), which suggested insufficient impedance matching compared to the proposed design which had a return loss of −49 dB. In a similar manner, the 2×2 MIMO antenna proposed for 28 GHz applications also realized a minimum return loss of −41.72 dB and wide bandwidth of 5.01 GHz however this occurred in the millimeter-wave band while the work presented here is limited to sub-6 GHz frequencies. Moreover, total return loss of −40 dB and bandwidth of 810 MHz was found for the square split-ring MIMO antenna which was lesser than the bandwidth achieved by proposed antenna. whereas the circular patch UWB MIMO antenna returned a bandwidth of 3.57 GHz with return loss = −39.5 dB; still, there is better matching in impedance and at wide operational bandwidth present for the proposed antenna as compared to circular patch antenna.

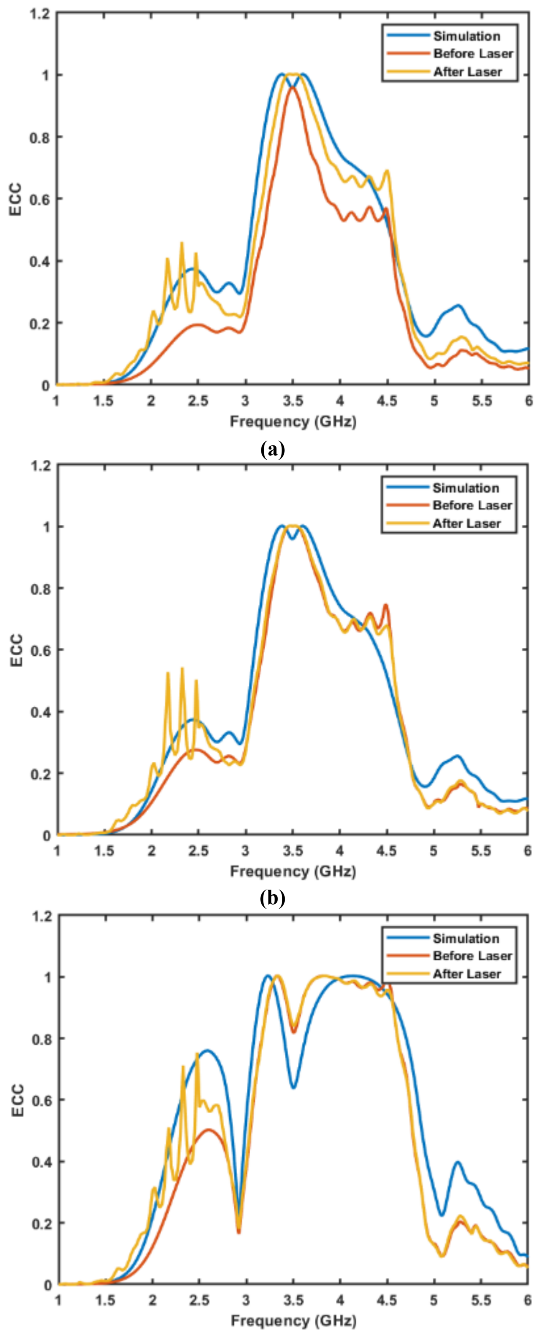


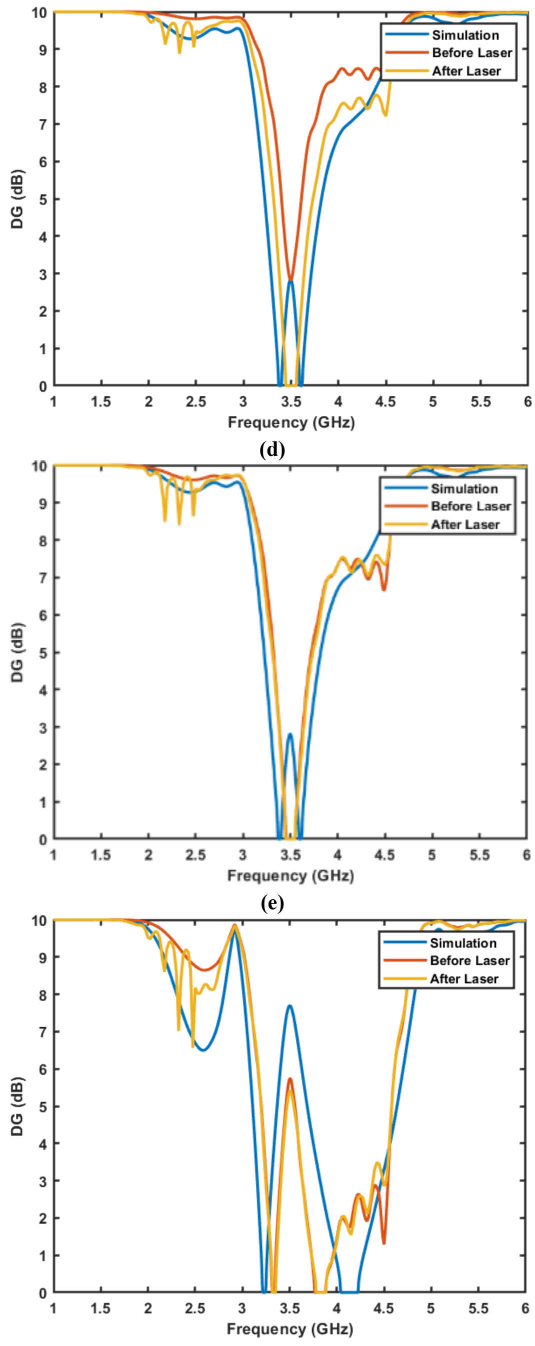


**Fig. (10) Measured parameters of the fabricated trapezoidal MIMO antenna before and after Nd:YAG laser treatment (a,b,c) ECC, (d,e,f) DG**

The result demonstrates that our proposed trapezoidal antenna design can achieve both an average bandwidth and a good 50Ω matching, with a compact structure to be used in sub-6 GHz 5G communication systems.

## 5. Conclusion

In this paper, a 4-port trapezoidal MIMO antenna with compound element for sub-6 GHz 5G applications is presented at its resonance frequency of f=3.545 GHz.

The main innovation consists of post-fabrication Nd:YAG laser treatment for performance improvement through surface modification. After surface profile of copper was evaluated by AFM showed 80% decrease in the surface roughness contributed directly to RF performance. Measured reflections after treatment showed excellent impedance matching with reflection coefficients of -27 dB and better, VSWR close to 1.1:1 and input impedances closely tuned to 50 Ω. MIMO diversity performance was recovered, and both ECC and DG matched simulations closely. These results confirm the excellent post-fabrication technique Nd:YAG laser treatment to remedy manufacturing imperfections, mitigate conductor losses and subsequently achieve optimal performance of high-frequency MIMO antenna systems for 5G applications.

**References**

[1] J.S. Aziz and A.S. Hussain, "Design of a compact MIMO antenna for 5G sub-6 GHz applications", *J. Eng., University of Baghdad*, 24(5) (2018) 45-60.

[2] J.S. Aziz and A.M. Al-Taei, "Design and Analysis of a Compact 4-Port MIMO Antenna for 5G Wireless Applications", *J. Eng., University of Baghdad*, 30(1) (2024) 115-130.

[3] A.S. Khoudair and A.H. Khidhir, "Improvement of Microstrip Patch Antenna Performance via Nd:YAG Laser Surface Treatment", *Baghdad Sci. J.*, 20(4) (2023) 1245-1254.

[4] C.A. Balanis, **"Antenna Theory: Analysis and Design"**, 4th ed., Wiley (NJ, 2016).

[5] I.N. Taban, A.H. Khidhir and A.A. Naser, "Design and Simulation of Planar Inverted F Antenna (PIFA) for Long Term Evolution Systems", *Al-Nahrain J. Sci.*, 25(4) (2022) 43-48.

[6] M.S. Rana et al., "An S-Band Microstrip Patch Antenna Design and Simulation", *Int. J. Electr. Electron. Eng.*, 10(4) (2022) 943-952.

[7] A.C. Bhosale et al., "Comprehensive Methodology for Advancing MIMO Circular Microstrip Patch Antenna Design", *J. Inform. Syst. Eng. Manage.*, 10(37) (2025) 637-649.

[8] M. Pant and L. Malviya, "Design of a high-gain, low-ECC 2x2 MIMO antenna for 28 GHz", *AEU Int. J. Electron. Commun.*, 175 (2024) 154130.

[9] Q.H. Kareem et al., "Optimize the Performance of Reconfigurable Antenna Based on Laser Treatment for Sub-6 GHz Applications", *Prog. Electromag. Res. Lett.*, 123 (2025) 95-103.

[10] I. Zewail, S. Mohsen and M.M. Zayed, "Design and Implementation of a Compact 20-Port Wideband MIMO Antenna Array for 5G/6G Indoor Base Stations", *Wireless Personal Commun.*, 146 (2026) 731-762.

[11] A.A. Khedr, B.E. Elnaghi and A.M. Mohamed, "Design of a Compact Dual Port 2x1 Ultra-Wideband MIMO Antenna for Radio Frequency Energy Harvesting", *Prog. Electromag. Res. M*, 128 (2024) 41-49.

[12] Z. Lei et al., "A Wideband Circularly Polarised High-Gain Antenna Using Array Technology and Truncated Dielectric Plates", *IET Microwaves Antenna Propag.*, 19(1) (2025) e70069.

[13] R.M. Elsagheer, "Study on bandwidth enhancement techniques of microstrip antenna", *J. Electr. Syst. Inform. Technol.*, 3(3) (2016) 527-531.

**Table (3) Comparative analysis of the proposed MIMO antenna**

| Parameter | Simulated | Laser Treatment | | Improvement |
|---|---|---|---|---|
| | | Before | After | |
| Peak ECC (Port 1–2) | ≈1.0 | ≈0.95 | ≈1.0 | Improved Curve Matching |
| Peak ECC (Port 1–4) | ≈1.0 | ≈0.85 | ≈0.98 | Peak Magnitude Accuracy Improved |
| Low-Band Correlation | 0.2–0.4 | <0.2 | ≈0.35 | Corrected Underestimation |
| DG at Resonance (Port 1–2 & 1–3) | 10→0 dB | 3 & 2.5 dB | ≈0 dB | Laser Tuning Effective |
| DG at Resonance (Port 1–4) | 10→5.5–6 dB | 4–5 dB | 5.5–6 dB | Notches Aligned |

  